

HARP COLLABORATION

HARP Note 03-004

July 22, 2003

Analysis of HARP TOF-WALL time calibration with cosmic rays

F. Bobisut, A. De Min, D. Gibin, A. Guglielmi,
M. Laveder, A. Menegolli* and M. Mezzetto

Dipartimento di Fisica "G.Galilei" and INFN, Padova, Italy

Abstract

An analysis of the systematic effects affecting the time calibration of the TOF-WALL detector with cosmic muons is given. An overall accuracy of about 60 ps on the time alignment procedure was found by studying time-of-flight of muons crossing the 2.5 cm overlap region between subsequent counters.

*Now at *Dipartimento di Fisica Nucleare e Teorica, Pavia, Italy*

1 Introduction

Several periods of cosmic rays muons data taking allowed to calibrate the whole TOF-WALL detector in HARP through the evaluation of the time calibration constants needed to align in time the 39 scintillation counters of the TOF-WALL. A dedicated analysis of the muons crossing the 2.5 cm overlap region between subsequent counters was accomplished in order to cross check the reliability of the calibration constants: the time-of-flight between two subsequent counters were expected, once inserted the calibration constants, to have zero mean value. The deviations from zero were studied accounting for the systematics introduced by the geometrical acceptance of the TOF-WALL convoluted with the detection efficiency of the counters, facing the TOF-WALL, used to trigger the cosmic muons. As a result a 60 ps precision of the time alignment procedure with cosmic muons was obtained.

1.1 The HARP TOF-WALL calibration procedure

As explained in a previous note [1], the time-of-flight in the HARP experiment is measured by the TOF-WALL, a set of 39 scintillation counters, arranged in three vertical walls, each consisting of 13 counters, placed at about 10 meters from the target, covering an overall area of $657 \times 243 \text{ cm}^2$ (see fig. 1).

The time calibration of the detector was accomplished with the analysis of cosmic-rays data collected in several periods during the data taking of the HARP experiment. The measured times $(t)_i^{PMT\ 0,1}$ of two PMT signals from the i -th counter needed to be corrected for the time misalignment introduced by signal-cables, PMTs, discriminators and for the staggering between counters and different position between the three TOF-WALL sections. Thus the corrected times $(t^C)_i^{PMT\ 0,1}$ are:

$$\begin{aligned}(t^C)_i^{PMT\ 0} &= (t)_i^{PMT\ 0} + (\Delta t_-)_i + \Delta_i \\ (t^C)_i^{PMT\ 1} &= (t)_i^{PMT\ 1} - (\Delta t_-)_i + \Delta_i ,\end{aligned}\tag{1}$$

where $(\Delta t_-)_i = < \frac{t^{PMT\ 0} - t^{PMT\ 1}}{2} >_i$ corrects for the relative timing of the two PMTs for center-crossing particle. The second correction term Δ_i is obtained with a step-by-step procedure:

1. the first step consists in aligning in time the counters within each one of the three walls by correcting the times measured by the two PMTs for the time-of-flight between the i -th counter and the Reference counter placed downstream the TOF-WALL:

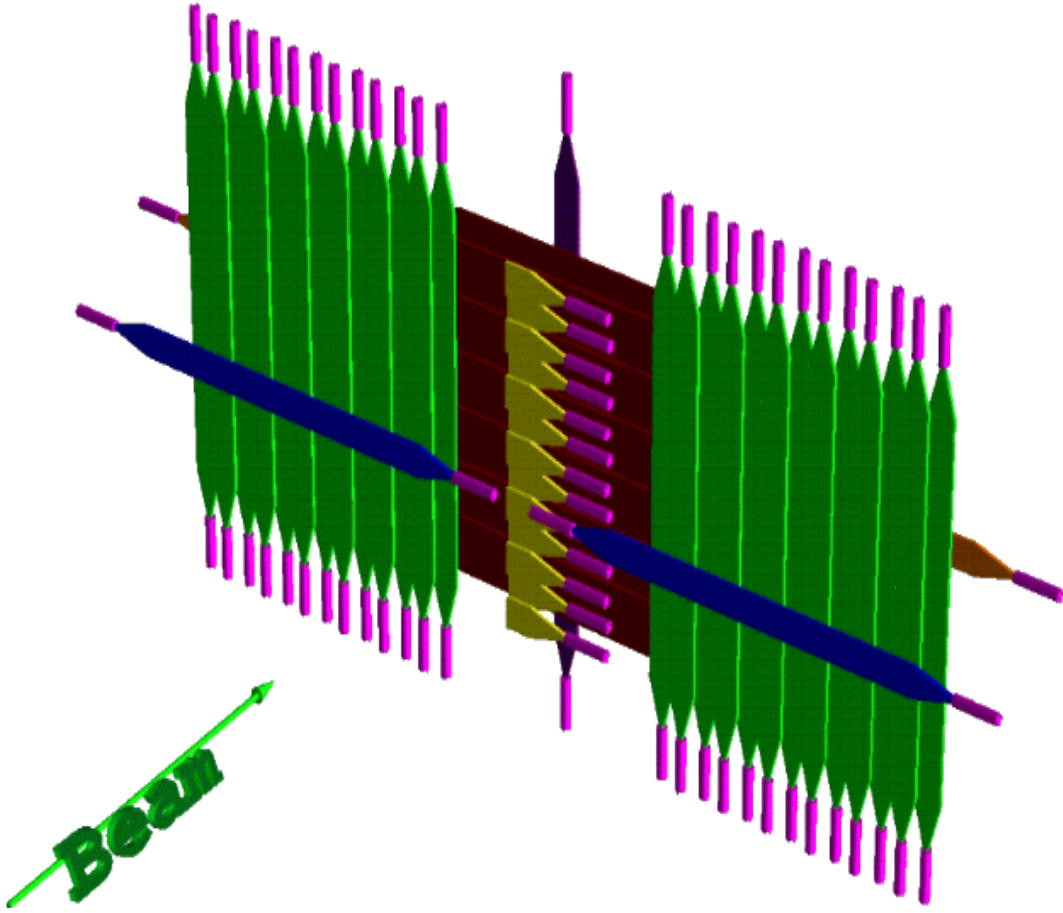


Figure 1: A sketch of the three walls composing the HARP TOF-WALL: left, center and right part.

$$TOF_i = \left\langle \left(\frac{t^{PMT\ 0} + t^{PMT\ 1}}{2} \right)_{REF} - \left(\frac{t^{PMT\ 0} + t^{PMT\ 1}}{2} \right)_i \right\rangle; \quad (2)$$

2. a second correction, $\Delta t_1 \sim 150$ ps, takes into account the difference of time-of-flight in alternate counters due to the staggering of the scintillators along the beam direction;
3. a further step consists in aligning in time the left (L) and the right (R) wall with respect to the central (C) one by using the muons crossing the small overlap regions between the central and the lateral walls in order to evaluate the offset:

$$\begin{aligned} \Delta t_{ref_L} &= tof(L - REF_L) - tof(C - REF_L) \\ \Delta t_{ref_R} &= tof(R - REF_R) - tof(C - REF_R); \end{aligned} \quad (3)$$

4. an average offset, $\Delta t_2 \sim 670$ ps, was then introduced to take into account the shifted position along the beam direction of the lateral walls with respect to the central wall.

The TOF-WALL time calibration relative to the HARP target position is then achieved by adding a term $TOF_{\beta=1}$, i.e. the time difference between the expected and measured time-of-flight of $\beta = 1$ particles between the counters near the target and the TOF-WALL. At the end of the correction procedure, the quantities Δ_i are given by:

$$\Delta_i = (TOF_i + \Delta t_1) + (\Delta t_{refL,R} + \Delta t_2) + TOF_{\beta=1}, \quad (4)$$

so that the corrected time of particles crossing the TOF-WALL, $(t^C)_i^{PMT\ 0,1}$, are determined.

1.2 The time calibration accuracy

The accuracy of the time calibration constants TOF_i can be evaluated taking into account the following factors:

1. the error on the calibration parameters of the three TDC modules; the maximum deviation from the linear fit of the calibration curves was found to be 10 ps;
2. the time walk corrections; the correction for the dependence of time on charge can be written as:

$$\delta t = W \left(\frac{1}{\sqrt{Q_0}} - \frac{1}{\sqrt{Q}} \right),$$

where Q is the charge, Q_0 is the peak of the charge distribution and $W = 11.4$ ns \cdot pC^{1/2} for all PMTs. The average error on δt is ~ 10 ps;

3. an average error of 5 ps introduced by the minimization procedure when the time distributions were fitted with a gaussian function;
4. dishomogeneity on selected cosmic rays μ 's angular distribution in the left and right walls, which gives a contribution to the error on the calibration parameters of about 50 ps. This is due to the reduced detection efficiency, i.e. the two PMT signal coincidence, at the extremities of the Trigger counters which favors more inclined trajectories with larger paths when the outer counter of the wall is involved (see the sketch in fig. 2). Both the left and right upstream Trigger counters were recuperated from a previous experiment.

As a conclusion, 60 ps of accuracy in the TOF-WALL time calibration constants Δ_i can be achieved with the cosmic muons calibration.

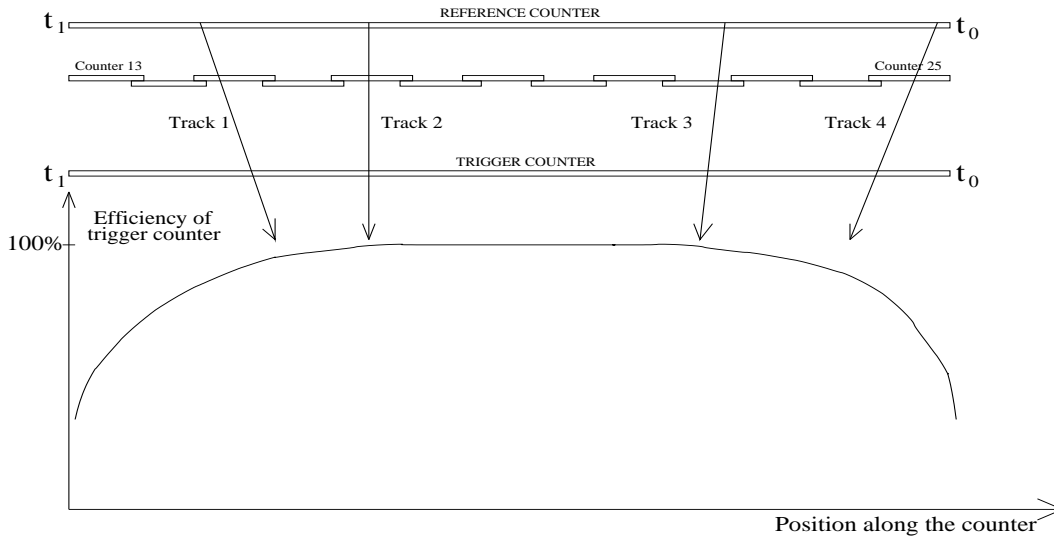


Figure 2: Cosmic rays tracks favored by the Trigger counter efficiency which introduces a difference in the corresponding t.o.f. (left-wall, top view).

2 Muons in the overlaps

As a cross-check of the results, the events crossing the left wall Reference counter in a 7 cm region centered on the overlap of 2.5 cm between two subsequent counters of the left wall were analyzed. Data were selected by requiring that the cosmic rays muons crossed four counters: the two in the overlap plus the Trigger one, placed upstream, and the Reference one placed downstream (see fig. 2). In addition, events with very low signals in both PMTs of the Reference counter, in correspondence with a large signal in both PMTs of the left wall counters, were excluded with an ADC cut: these events hit the edge of the Trigger counters and would require large time-walk corrections. Corrections for time walk effect, as well as for time alignment inside a wall, $(\Delta t_-)_i$ and TOF_i , were used. The distributions of times-of-flight between two subsequent counters built in this way were expected to have zero mean value, because of the time alignment of the counters. Unexpectedly these distributions have mean value even 100 ps different from zero (see tab. 1), in some cases much above the evaluated precision, of the order of 60 ps (see par. 1.2).

2.1 Charges and times in the overlap region

To understand the problem, the analysis of the cosmic rays event crossing the overlaps was repeated changing the previous selection conditions:

- the region in the Reference counter centered on the overlaps was reduced to 5.5 cm;

Counters in overlap	Mean t.o.f. (ps)
13-14	104
15-14	-87
15-16	71
17-16	-20
17-18	26
19-18	-26
19-20	-1
21-20	-33
21-22	-9
23-22	9
23-24	-55
25-24	53

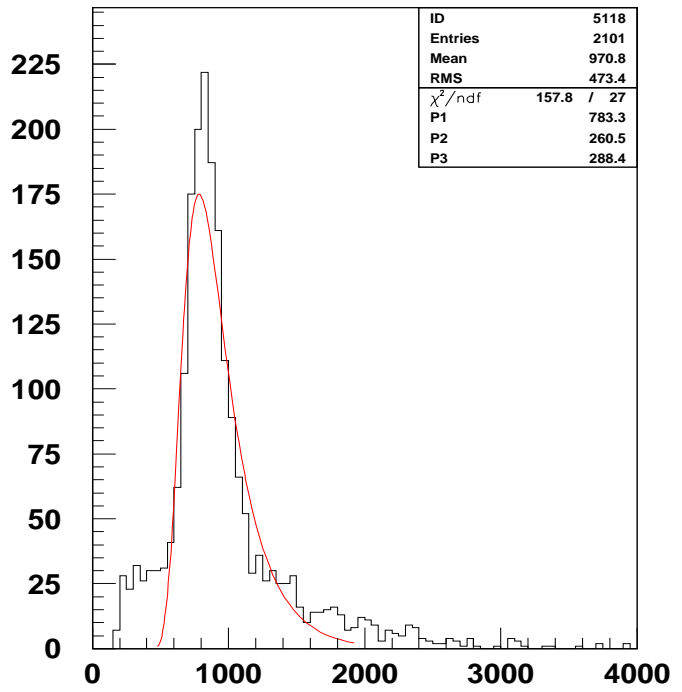
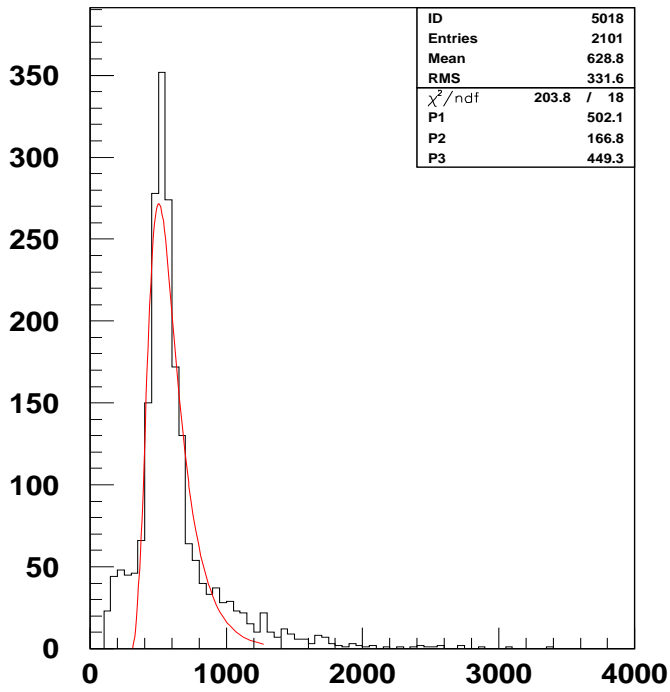
Table 1: Mean values of the times-of-flight in the overlap region between two subsequent counters of the left wall of TOF-WALL detector.

- no time walk correction of the times-of-flight was used;
- no time calibration constants were inserted.

Then the ADC distributions for each of the two PMTs for all counters of the left wall and the time-of-flight between the wall counters and the downstream Reference one were built:

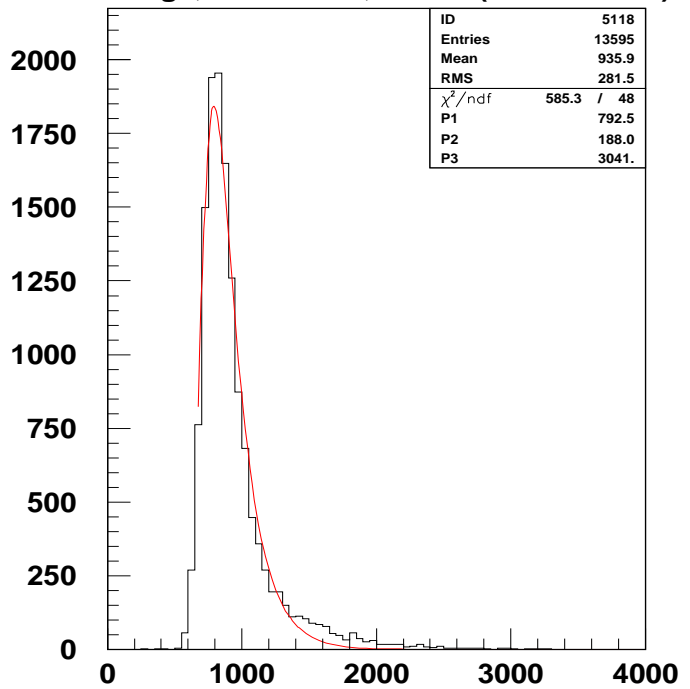
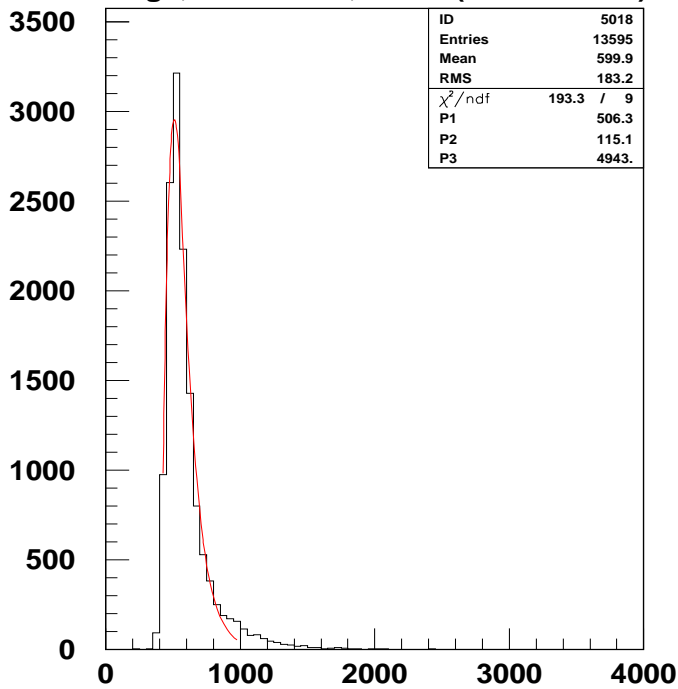
- the distributions of times-of-flight between the wall counters and the Reference one show how the mean values of the t.o.f. evaluated for the same counters at the two overlap regions were different, even by more than 200 ps (see tab. 2);
- the corresponding charge distributions (see fig. 3) show tails at low ADC values, due to events which hit the edge of the counters: these events, that were not evident for tracks crossing the counters at their centers, were excluded from the following analysis, rejecting the events with an ADC value lower than an RMS value from the mean value of the fitted Landau.

These differences of times-of-flight at the two sides of the counters were reduced down to 70 ps with the ADC event selection described above and they resulted unaffected by the insertion of time walk corrections and time calibration constants (see tab. 3 and fig. 4). However a systematic decrease of the times-of-flight from counter 13 to 18 and then an



Charge, counter 18, PMT0 (QDC counts)

Charge, counter 18, PMT1 (QDC counts)



Charge, counter 18, PMT0 (QDC counts)

Charge, counter 18, PMT1 (QDC counts)

Figure 3: ADC distributions for the two PMTs of counter 18 of left wall, for events crossing the region of overlap between counters (above), and crossing counters at their centers (below).

Counter	Overlap #1 (ns)	Overlap #2 (ns)	t.o.f. difference (ps)
14	-0.803	-0.914	-111
15	0.041	-0.162	-203
16	-2.021	-1.955	66
17	-0.367	-0.228	139
18	-0.549	-0.474	75
19	1.636	1.667	31
20	-1.353	-1.321	32
21	-2.740	-2.771	-31
22	-5.215	-5.222	-7
23	-5.298	-5.372	-74
24	-3.405	-3.515	-110

Table 2: Times-of-flight between a counter of the left wall and the Reference one in the two windows centered in the overlap between two subsequent counters. No time walk corrections and time calibration constants were inserted.

increase from counter 21 to 24 going from the the left side to the right side of the counters was observed. The time-of flight between two subsequent counters in the overlap region, with the same conditions, were still different from the expected zero mean value, even if in the first half of the left wall an improvement is visible (see tab. 4). Since the selection criteria were the same for the two regions of overlap, the effect could be possibly due to:

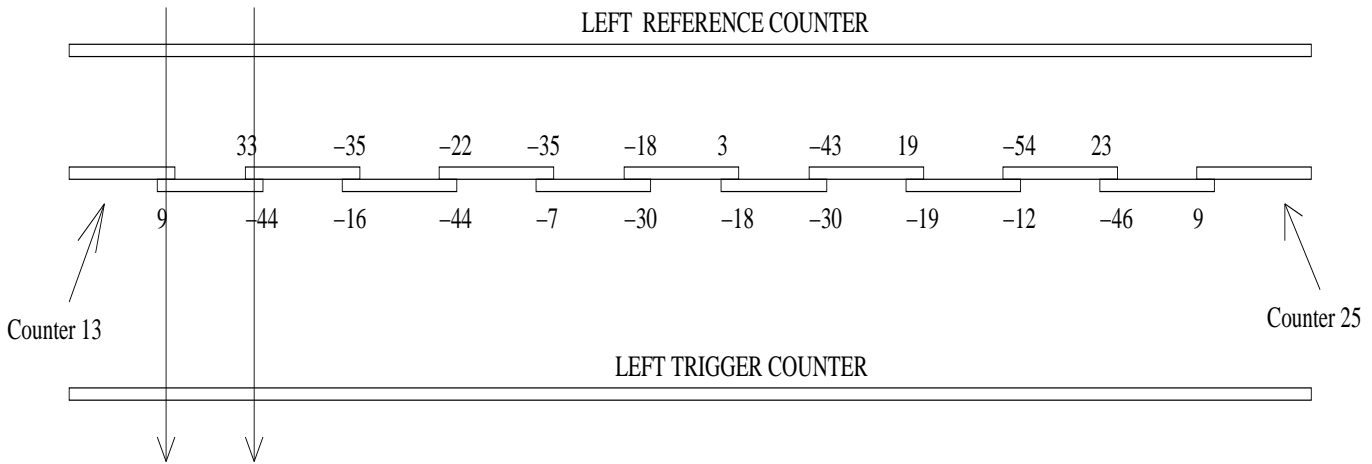
- A. the size and/or the position of the time window on the Reference counter by means of which the region of overlap between the counters were selected;
- B. the efficiency of the Trigger counter placed upstream the left wall.

2.2 Geometry and trigger efficiency effects

As shown in fig. 5 the windows centered in the overlaps between left wall counters select cosmic ray tracks with different slopes, according to the zone of the overlap. In fact the inclined track selection is determined by the geometrical acceptance of the overlap convoluted with the upstream Trigger counter efficiency, which decreases moving from the center to the edges of the counter, favoring the particles passing through the center of the Trigger counter (see fig. 2). These efficiency losses, measured in previous laboratory tests, can be recognized here from the distribution of μ hit position X along the Trigger slab which is obtained from the time difference of the two PMT signals, $(t_1 - t_0)/2$ (see

Counter	Overlap #1 (ps)	Overlap #2 (ps)	t.o.f. difference (ps)
14	9	-44	-53
15	33	-35	-68
16	-16	-44	-28
17	-22	-35	-13
18	-7	-30	-23
19	-18	3	21
20	-18	-30	-12
21	-43	19	62
22	-19	-12	7
23	-54	23	77
24	-46	9	55

Table 3: Times-of-flight between a counter of the left wall and the Reference one in the two windows centered in the overlap between two subsequent counters. Time walk corrections and time calibrations constants TOF_i were inserted.



Cosmic rays crossing the overlaps between counters.

Figure 4: Geometry of the overlaps between counters in the left wall. On each overlap region the time-of-flight between the corresponding counter and the Reference one is shown (in ps).

Counters in overlap	Mean t.o.f. (ps)	Mean t.o.f. (ps), cut ADC
13-14	104	79
15-14	-87	-69
15-16	71	33
17-16	-20	-35
17-18	26	16
19-18	-26	-18
19-20	-1	-25
21-20	-33	0
21-22	-9	-18
23-22	9	32
23-24	-55	-68
25-24	53	53

Table 4: Mean values of the times-of-flight in the overlap region between two subsequent counters of the left wall of TOF-WALL detector.

fig. 6). In particular a substantial difference of detection efficiency of the two PMTs for particle crossing in opposite counter extremities (for $|(t_1 - t_0)/2| \simeq 8$ ns) can be detected from the observed left-right asymmetry (see fig. 6). As a result tracks crossing the overlap 13-14 are on average more inclined than the ones passing through the overlap 14-15 (see fig. 5). This effect gradually decreases going to the overlap zones at the center of the wall, where the trigger efficiency is almost the same for all trajectories.

These geometrical effects, convoluted with trigger efficiency, can be visible also in the distribution of the time difference $(t_1 - t_0)/2$ of the two PMTs of the Reference counter inside the selected time window which determine the 5.5 cm overlap regions (see fig. 7). The 13-14 overlap favors events with small t_0 and high $(t_1 - t_0)/2$, the next one (14-15) events with high t_0 and small $(t_1 - t_0)/2$, and so on alternatively. This effect was not detected in the counters in the central part of the wall (see overlap 17-18 and 20-21 in fig. 7). It follows that for very inclined tracks as those selected by the overlap zones, the geometrical acceptance (with the alternation of negative and positive slopes in $(t_1 - t_0)/2$ distributions) and the Trigger counter efficiency (the slopes in $(t_1 - t_0)/2$ distributions differ in value) modify the time-of-flight values measured.

These systematic time-of-flight effects were also confirmed by studying the values of the time-of-flight between the left wall counters and the Reference one, and the correlated charge, as a function of the position of the track along the Reference counter in the area faced to the 21 cm width of the interested left wall counter, where cosmic rays

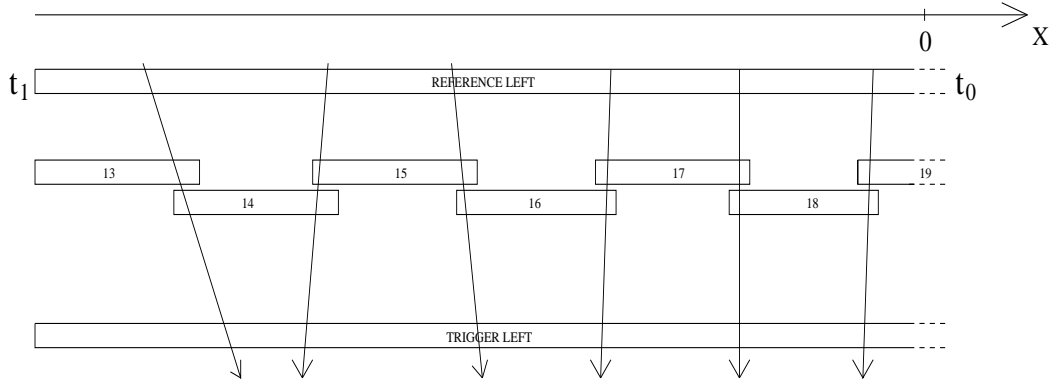


Figure 5: Cosmic ray tracks selected by the zone of overlap. The X -coordinate along the Reference counter and Trigger counter is evaluated by the two PMT time difference $(t_1 - t_0)/2$. The $X = 0$ position refers to the center of the Reference/Trigger counter.

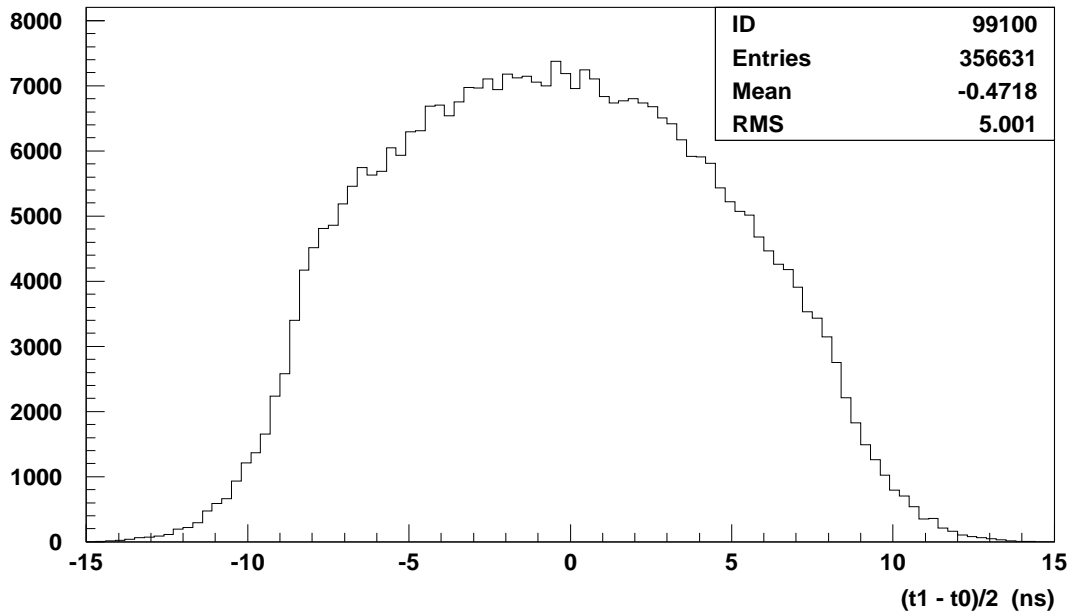


Figure 6: The $(t_1 - t_0)/2$ distribution of the two PMT time difference of the left wall Trigger counter.

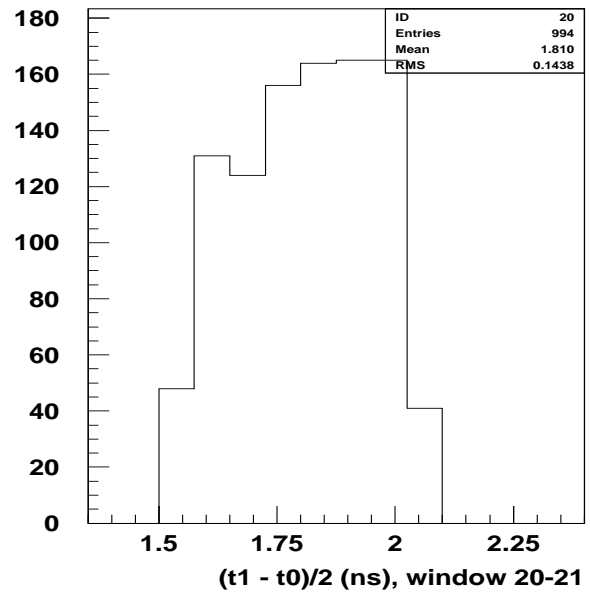
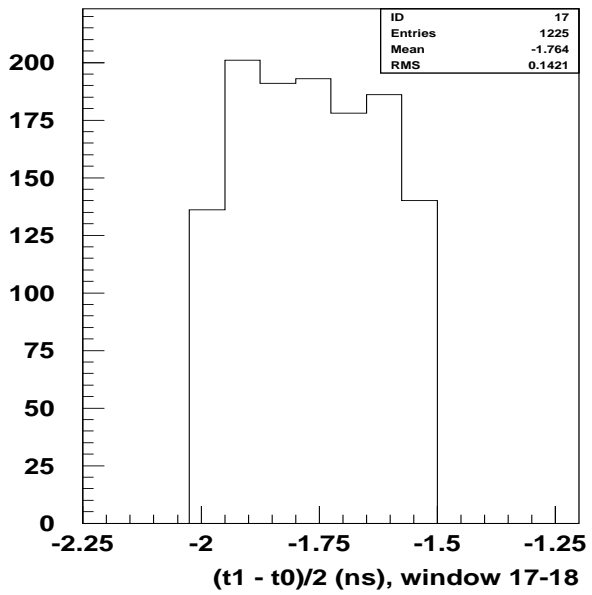
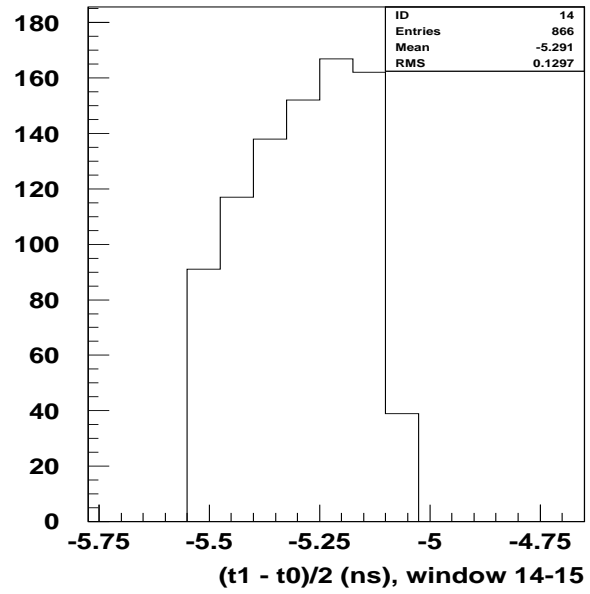
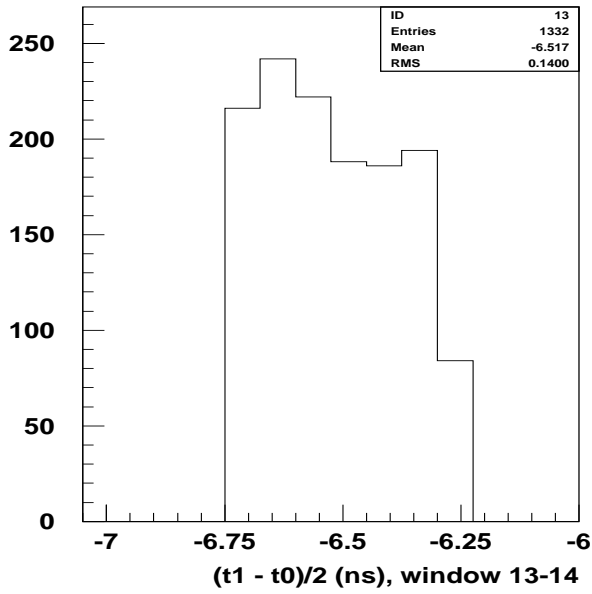


Figure 7: The $(t_1 - t_0)/2$ distribution of two PMTs of the Reference counter in the first two subsequent zones of overlap between left wall counters (counters 13-14 and 14-15), and in two zones of overlap at the center of left wall (counters 17-18 and 20-21).

tracks crossing the overlaps were rejected. The crossing position was reconstructed from $(t_1 - t_0)/2$ PMT time difference of the Reference counter. As a result (see fig. 8) time-of-flight in counters 13÷16 (22÷25) decreased (increased) with the hit position selected in the Reference counter going from the the left side to the right side of the counters, showing up to 90-100 ps of difference. On the contrary no evidence of similar systematics effects was observed for the central counters, 17÷21, of the left wall. However the largest part of event statistics resulted concentrated in the ~ 10 cm central counter region, where the observed differences on t.o.f. are well below 50 ps.

At the same time the corresponding charge as a function of the position of the hit along the counter (see fig. 9) is correlated with respect to the time-of-flight, with ADC values increasing where t.o.f. increases and vice versa; the relative variations go from a 3% (central counters) to 6% (outer counters). It should be noticed that this dependence of the ADC values on the position along the counters is not due to time walk effects, the corrections for which were previously used on the left wall counters, but to the convolution of both geometrical and trigger efficiency effects for very inclined muon tracks crossing different regions of the left wall.

2.3 Right wall

A preliminary analysis of cosmic ray tracks crossing the overlaps between subsequent counters of the right wall (TOF-WALL counters 25÷38) was made in order to investigate the geometrical and trigger efficiency effects in the right wall.

With the same selection criteria of sec. 2.1 (ADC cuts, insertion of time walk corrections and time calibration constants TOF_i), time-of-flight in the overlap region between two subsequent counters of the right wall still differed from the expected zero mean value (see tab. 5). The time-of-flight between the right wall counters and the Reference one systematically decreases (counters $\sim 27\div 29$) and then increases (counters 34÷37, except 36) going from the the left side to the right side of the counters (see tab. 6).

3 Conclusions

The analysis of the cosmic muon in the overlap counters of the TOF-WALL allowed to measure and test the reliability of the calibration time constants of the TOF-WALL counters. As expected a 60 ps of precision was found, essentially due to the geometrical acceptance and efficiency of the upstream counters used to trigger the cosmic-muons.

Counters in overlap	Mean t.o.f. (ps), cut ADC
26-27	70
28-27	-22
28-29	18
30-29	-31
30-31	-10
32-31	5
32-33	-16
34-33	-30
34-35	-68
36-35	-8
36-37	-76
38-37	48

Table 5: Mean values of the time-of-flight in the overlap region between two subsequent counters of the right wall of TOF-WALL detector.

However these systematics are clearly affecting only the outer counters of the left and right part of the TOF-WALL.

References

- [1] F. Bobisut et al., “*The HARP TOF-WALL performance and time calibration*”, INFN/BE-02/03, HARP Note 02-007.

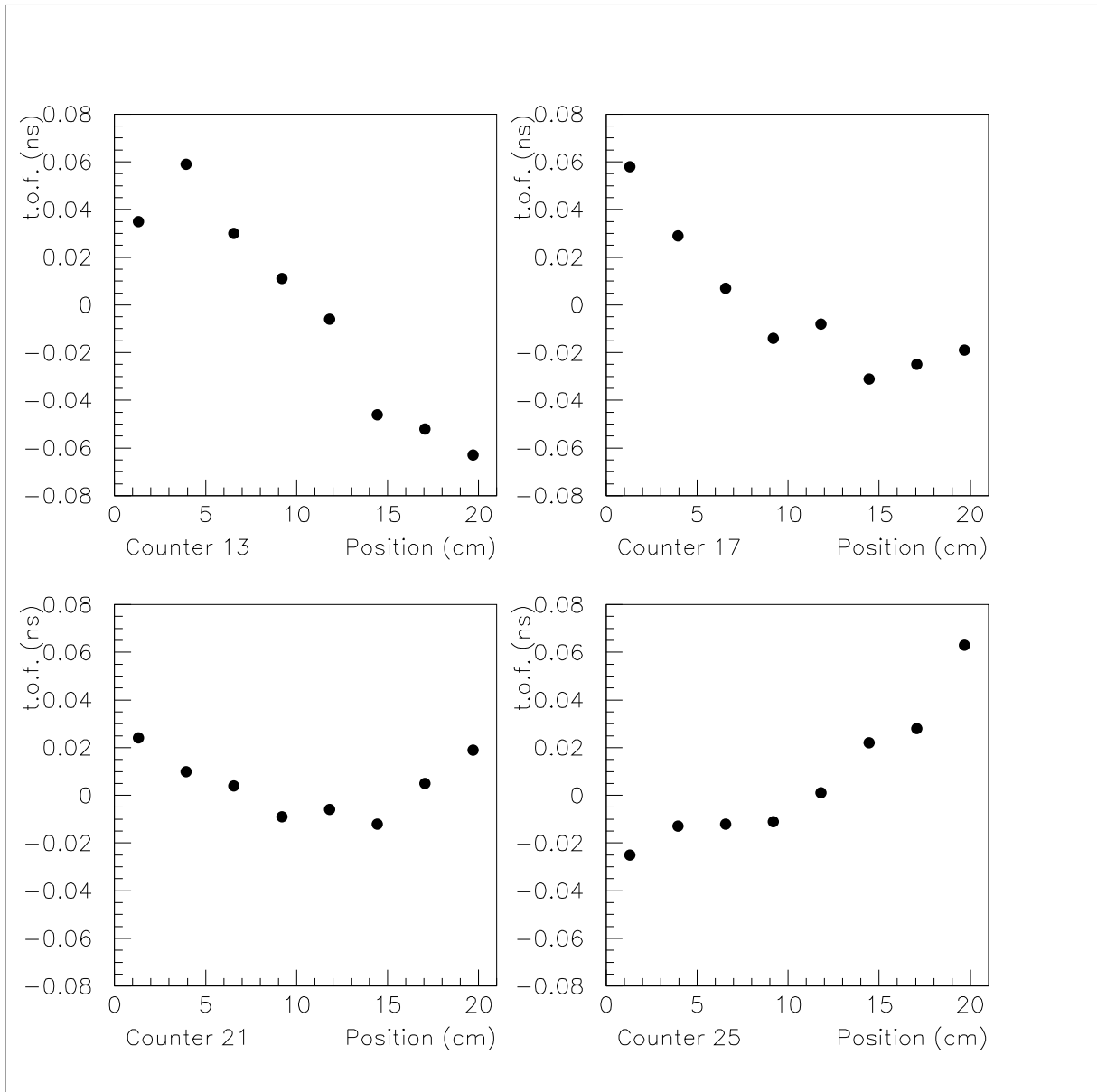


Figure 8: Time-of-flight between the left wall counters and the Reference one, as a function of the position X of the track along counters 13 , 17, 21 and 25.

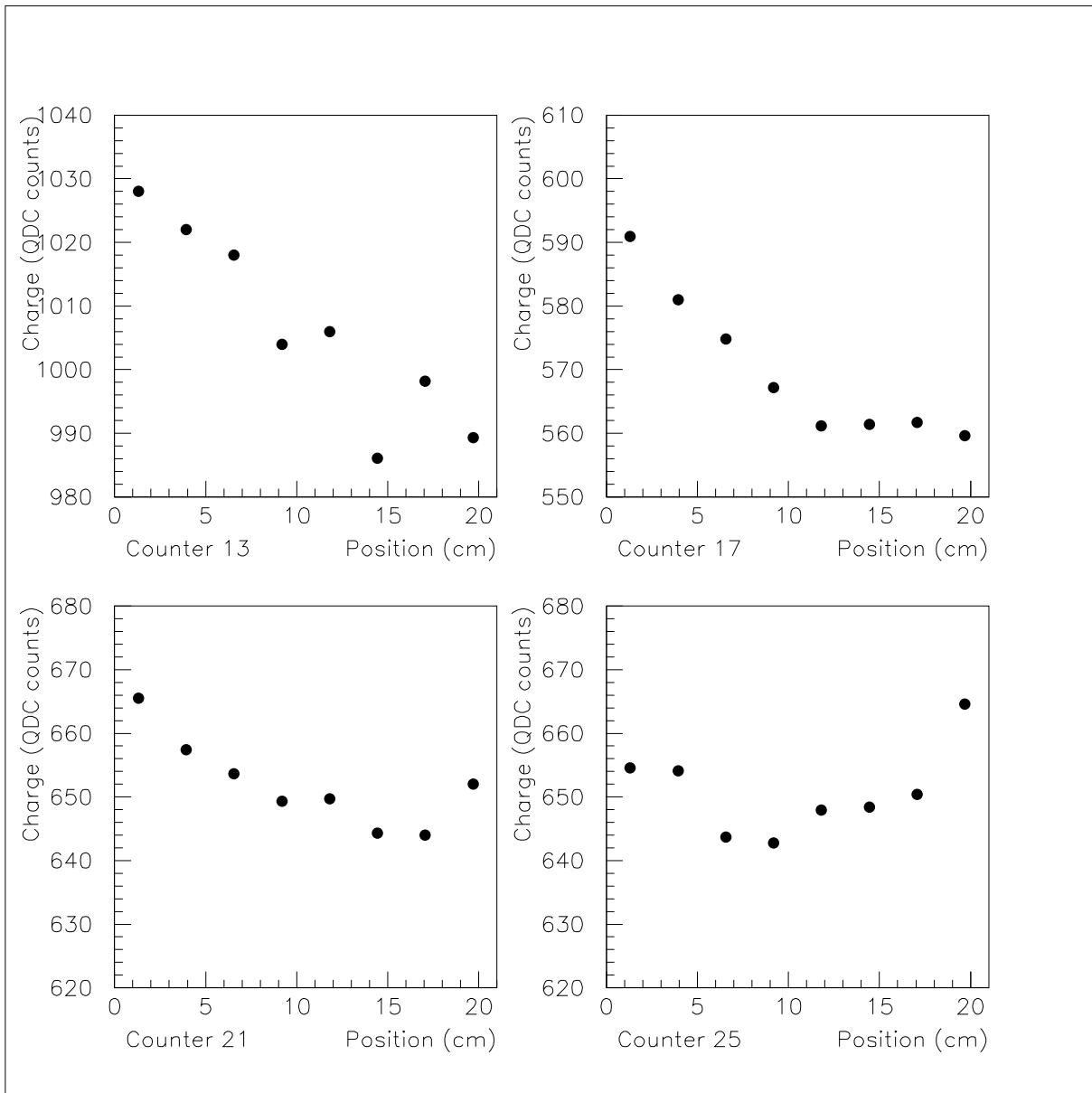


Figure 9: ADC counts (PMT 0) as a function of the position X of the track along counters 13, 17, 21 and 25.

Counter	Overlap #1 (ps)	Overlap #2 (ps)	t.o.f. difference (ps)
27	6	-41	-47
28	-14	-25	-11
29	-10	-74	-54
30	-25	-18	7
31	-32	-8	24
32	-6	1	7
33	-34	-65	-31
34	-46	1	47
35	-74	-34	40
36	-32	-83	-51
37	-70	0	70

Table 6: Time-of-flight between a counter of the right wall and the Reference one in the two windows centered in the overlap between two subsequent counters.